RSC Advances

ROYAL SOCIETY
OF CHEMISTRY

www.rsc.org/advances

RSC Advances

PAPER

Magnetic nano catalyst for the synthesis of maleimide and phthalimide derivatives.

Pranila B. Thale[a], Pravin N. Borase[a], and Ganapati S. Shankarling[a]

An efficient and green protocol for the synthesis of *N*-aryl maleimide and phthalimide derivatives is developed. The high efficiency of the catalyst was observed due to homogeneous distribution of the nanoparticles. Catalyst was fully characterised by physicochemical methods such as IR spectroscopy, scanning electron microscopy (SEM), transmission electron microscopy (TEM), X-ray diffraction, dynamic light scattering (DLS), energy dispersive X-ray spectrum and zeta potential measurement techniques. The ease of separation of the catalyst from the reaction mixture and its high activity are eco-friendly attribute of   this   system.

Introduction:

Nanoparticles have emerged as an important tool in catalysis[1,2]. It acts as a bridge between homogeneous and heterogeneous catalysis. Nanoparticles can get homogenised in reaction mixture during organic synthesis to increase catalytic efficiency and it can be easily separated by means of centrifugation or external magnetic field[3]. Since past few years, catalyst supported over magnetic nanoparticles have gained considerable attention in C-X coupling and other organic reactions[4–8]. Hazardous mineral acids are always in demand for numerous acid catalysed reactions for their excellent catalytic performance[9]. However, their sepraration from reaction mixture exhibits limitation on their use due to enviormental concerns. Such mineral acids after supporting over magnetic nanoparticles, can be eaisly seperated from reaction mixture without hampering their catalytic activity, which makes the protocol more cost effective and environmentally benign. *N*-Substituted imide derivatives find wide application in medicinal chemistry[10,11] biology[12,13] material science and polymer chemistry[14]. Maleimides are backbone of peptide-conjugate haptens, immune conjugates, and enzyme inhibitors[15]. In organic synthesis, imide derivatives play a vital role for protection of amino group[16]. Despite their wide application, availability of environmentally benign, inexpensive synthetic protocol for the preparation of imides is limited.

[a]Dyestuff Technology Department, Institute of Chemical Technology, Mumbai 400019, India.

Corresponding author: Tel: 91-22-33612708, Fax: +91-22-33611020, E-mail address: gsshankarling@gmail.com

The conventional methods for synthesis of imide derivatives are the dehydrative condensation of anhydride and amine in the presence of sulfuric acid[17] and *N*-alkylation of imides promoted by PPh_3 in presence of alcoholic media[18]. These conventional protocol suffer drawback like high temperature and longer reaction time. Several attempts have been reported using ionic liquids[19],[20] as well. Unfortunately, they also suffer from longer reaction time and tedious product isolation methods. Hence, there is a need for development of protocol for the synthesis of imide derivatives with a shorter reaction time and easy separation of products from reaction mass. In current protocol, we have introduced sulphuric acid functionalised silica supported over magnetite nanoparticles. It provides easy separation of catalyst from reaction mass and its recyclability induces cost effectiveness to the system.

<center>**<Insert Scheme: 1>**</center>

Results and discussion:

In the present work, we have reported a simple, efficient and practical approach for the synthesis of *N*-aryl imide derivatives. We have used phthalic anhydride, aniline as standard substrates to screen a suitable solvent for the reaction. Among the tested solvents, ethanol was the most effective reaction medium for *N*-insertion reaction (Table 1, Entry 6). Low yield of the target product was obtained when EDC, DMF, toluene, acetone were used as solvents. When the reaction was carried out on bare magnetite nano particle Fe_3O_4 (Table 1, Entry 4), as well as on bare silica coated nano particle $Fe_3O_4@SiO_2$ (Table 1, Entry 5), it resulted in poor yield. Whereas, it gave a good yield with sulfonic acid functionalized silica coated magnetite nano catalyst. To determine the catalyst loading model reaction of phthalic anhydride and aniline in ethanol was performed. The reaction occurred smoothly in presence of 20 wt.% of $Fe_3O_4@SiO_2\text{-}SO_3H$, affording a single product (Table 2, entry 4) in 89% yield. Increasing the amount of catalyst, to more than 20 wt.% showed no substantial improvement in the yield. It is worthy to mention that, we examined the model reaction without any catalyst in ethanol at reflux temperature and the product yield did not increased beyond 29% even after prolonged heating (Table 1, Entry 1). The optimized reaction conditions include 3.37 mmol of phthalic anhydride, 3.37 mmol of aniline and 20 wt.% of $Fe_3O_4@SiO_2\text{-}SO_3H$ in ethanol at $80^\circ C$. Furthermore, for comparison the model reaction was carried out using amberlyst 15 and silica sulfuric acid under the similar condition which gave the desired product in 81% and 77% yield respectively (Table 1, Entries 2 and 3) after 8 hr. of heating. This suggests that, catalyst plays a major role in the reaction. The reaction was faster in case of $Fe_3O_4@SiO_2\text{-}SO_3H$ catalyst because of acid active sites and higher surface area of the catalyst due to its nano form. To investigate the effect of electron donating and withdrawing group on the rate of reaction, we have studied

different anhydride with various aromatic primary amines (Table 3). In case of electron donating substituent the reaction was faster and gave better yield whereas, reaction afforded moderate to good yield when an electron withdrawing substituent was present on the aromatic amine. The proposed reaction mechanism of the reaction using catalyst is depicted in fig.1.

The catalyst was easily separated from the reaction mixture by magnetic separation method. It was successfully recycled up to six runs. The catalyst performs well with high turnover number (TON) and turn over frequency (TOF), which indicates that the catalyst is highly stable and efficient. The quanta of acid sites determined on the catalyst is 0.4 mmolg^{-1}.

Table 1: Effect of solvent and catalyst on the synthesis of *N*-phenyl phthalimide.

Entry	Catalyst	Wt.%	Solvent/ Temp	Time (hr.)	Yield (%)^a
1	-	-	Ethanol/80°C	4	29%
2	Amberlyst 15	20%	Ethanol/80°C	8	81%
3	Silica sulfuric acid	20%	Ethanol/80°C	8	77%
4	Fe_3O_4	20%	Ethanol/80°C	1	traces
5	$Fe_3O_4@SiO_2$	20%	Ethanol/80°C	1	traces
6	$Fe_3O_4@SiO_2$-SO_3H	20%	Ethanol/80°C	1	89%
7	$Fe_3O_4@SiO_2$-SO_3H	20%	Toluene/ 80°C	1	72%
8	$Fe_3O_4@SiO_2$-SO_3H	20%	DMF/80°C	1	70%
9	$Fe_3O_4@SiO_2$-SO_3H	20%	EDC/80°C	1	30%
10	$Fe_3O_4@SiO_2$-SO_3H	20%	Acetone/55°C	1	32%

^{a}isolated yields

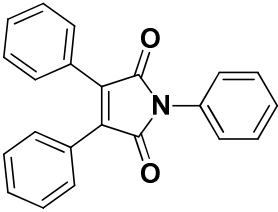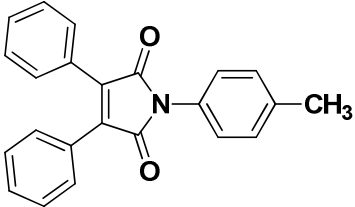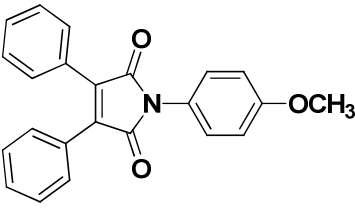Reaction condition: phthalic anhydride: 3.37 mmol; aniline: 3.37 mmol; Solvent: 5ml
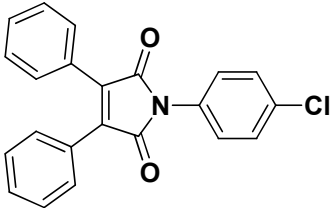
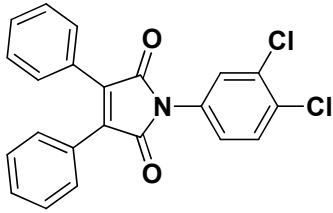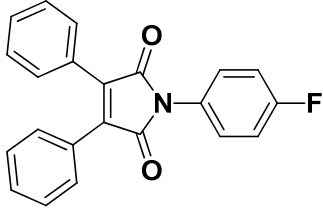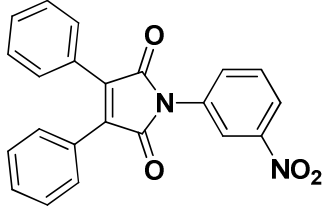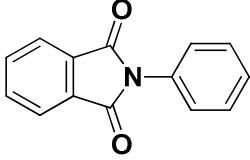Table 2: Effect of catalyst loading (wt.%) on the synthesis of *N*-phenyl phthalimide.
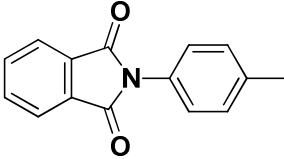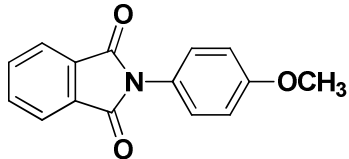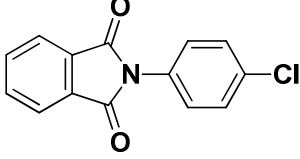
Entry	Catalyst wt.%	Time (hr.)	Yield(%)[a]
1	5%	5.0	60%
2	10%	3.0	67%
3	15%	2.5	74%
4	20%	1.0	89%
5	25%	1.0	89%
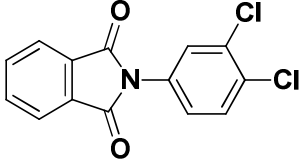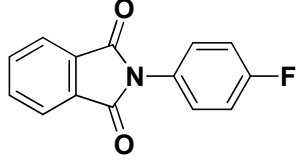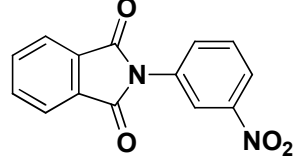
[a]isolated yield

Reaction condition: phthalic anhydride: 3.37 mmol; aniline: 3.37 mmol; Solvent: ethanol: 5ml; Temp = 80 $^\circ$C.

Table 3: The synthesis of *N*-aryl imide derivatives in presence of $Fe_3O_4@SiO_2-SO_3H$.

Entry	Product	Time	Yield (%)[a]	TON[b]	TOF[c] (min.$^{-1}$)
A		2 hr.	84%	41.96	0.34
B		2 hr.	86%	42.96	0.35
C		1 hr. 30 min	88%	43.96	0.32
D		2 hr. 15 min	81%	40.46	0.29

E		2 hr. 45 min	77%	38.46	0.23
F		2 hr. 15 min	80%	39.96	0.29
G		4 hr.	76%	37.96	0.15
H		1 hr.	89%	75.11	1.25
I		1hr.	90%	75.95	1.26
J		45 min	91%	76.80	1.70
K		1hr. 30 min	81%	68.36	0.75

RSC Advances Accepted Manuscript

L	(structure)	1hr. 45min	80%	67.51	0.64
M	(structure)	1hr. 30 min	78%	65.83	0.73
N	(structure)	2 hr. 30 min	77%	64.98	0.43

[a]isolated yield

[b]TON= turn over number

[c]TOF= turn over frequency

Reaction condition = Temp. 80°C; catalyst loading: 20 wt.% ; Reaction medium: 5 ml ethanol

Characterisation of the catalyst:

TEM image of the catalyst display dark Fe_3O_4 core surrounded by a lighter amorphous silica shell as shown in fig. (2b) which confirms that the catalyst has been encapsulated by a thin layer of silica particles and it has average particle size of 30 nm. The energy dispersive spectrum indicated the presence of Fe, Si and S (fig.12 supporting information). SEM image of $Fe_3O_4@SiO_2$-SO_3H nanoparticles is shown in fig. (2a) which shows spherical morphology and it has marked tendency to form large aggregates. The clustering tendency was observed because of weak hydrogen bonding forces between $Fe_3O_4@SiO_2$-SO_3H and magnetic characteristic of nanoparticles.

The XRD analysis of Fe_3O_4, $Fe_3O_4@SiO_2$, $Fe_3O_4@SiO_2$-SO_3H has been done and its comparative spectra is depicted in fig.3. The XRD spectrum of Fe_3O_4 clearly matches with those of the literature report [21]. The XRD pattern of $Fe_3O_4@SiO_2$, $Fe_3O_4@SiO_2$-SO_3H shows broad band at 2θ =20-24° which is due to the presence amorphous silane shell formed around the magnetic core. There is no any other appreciable shift in the peak positions,which indicates the structural stability of magnetite nanoparticles. The zeta potential of the Fe_3O_4, $Fe_3O_4@SiO_2$ and $Fe_3O_4@SiO_2$-SO_3H samples has been performed to determine the surface modification of the nanoparticle. The observed zeta potential of the Fe_3O_4 and $Fe_3O_4@SiO_2$ were about -45mV and -120mV (fig.8 & 9 supporting information) respectively, which explains that the surface modification of the nano Fe_3O_4 has occurred and it is in good agreement with the literature data[22].

The zeta potential distribution for $Fe_3O_4@SiO_2$-SO_3H is positively charged at 25.3mV (82%) and 95.5 mV (18%). It is because of presence of H^+ ion on the surface of the catalyst fig. 4. To determine percentage average particle present in the sample, dynamic light scattering measurement were carried out as shown in fig. 5 and the observed results were similar to the literature report[23]. For this, aqueous stock solution (1 mg/ml of water) was prepared in ultrasonic bath for 30 min.

The IR spectroscopy shows band between 637-410 cm^{-1} which corresponds to stretching vibration of Fe-O bond[24]. The band at 1080 cm^{-1} corresponds to Si-O stretching vibration fig. 6b. The weak band at 814 cm^{-1} is observed for Si-O-Fe bond fig. 6b which indicates immobilisation of silica on the surface of Fe_3O_4 nanoparticle[25]. This band is shifted to 807 cm^{-1} in case of $Fe_3O_4@SiO_2$-SO_3H fig 6c. The fig. 6a and 6b shows broad peak between 3000-3400 cm^{-1} and a sharp peak around 1630 cm^{-1} for the presence of adsorbed water. The absorption band at 1128 cm^{-1} corresponds to stretching of S-O bond fig 6c, which justify the presence of the sulfonic acid group on its surface. The broad absorption at 3453 cm^{-1} and sharp peak at 1624 cm^{-1} corresponds to stretching vibration of OH group in the SO_3H fig. 6c.

<Insert Figure: 2>

<Insert Figure: 3>

<Insert Figure: 4>

<Insert Figure: 5>

<Insert Figure: 6>

Recyclability study:

The catalyst recyclability study was carried out on phthalic anhydride 3.37 mmol, aniline 3.37 mmol and catalyst (20 wt.%) in 5 ml ethanol at $80^\circ C$. The results are summarised in fig. (7). After completion of the reaction, catalyst was separated by an external magnet, washed with acetone and dried at $60^\circ C$ for 1 hr. The recovered catalyst was then used for next batch. It was observed that catalyst could be recycled efficiently up to six runs. SEM and TEM images of the recycled catalyst were taken fig. (8a and 8b) which show that, the structural and morphological properties of the catalyst remain unaltered even after 6th recycle. The comparative IR spectra of fresh and reused catalyst shows that there is no change in functional group values (fig.7 supporting information)

<Insert Figure: 7>

<Insert Figure: 8>

Determination of acidic sites:

The surface-bound acidic protons were ion exchanged with a brine solution by sonicating the $Fe_3O_4@SiO_2-SO_3H$ catalyst for 24 hr. The catalyst was separated magnetically, the brine solution was decanted and titrated with 0.1N NaOH solution to determine the loading of acid sites on the catalyst. The H^+ ions loading was found to be 0.40 mmol g^{-1}.

Experimental:

Materials and Methods:

TEM studies of the nano catalyst were carried out with JEOL JEM-2100 instrument. SEM micrographs and EDXS data were obtained on JEOL JSM 6380LA instrument. The XRD study was performed on a Bruker AXS powder diffractometer D8 with Cu-kα (1.54°A). The FT-IR spectra of the catalyst were measured with KBr pellets using a Bruker-VERTEX 80v vacuum FTIR spectrometer and the IR spectra of the synthesized compound were recorded on Jasco FT-IR ATR-PRO/4100 spectrophotometer. 1H NMR spectra were recorded on Bruker 400 MHz Spectrometer and Agilent 500 MHz spectrometer in $CDCl_3$ solvent. Mass spectral data were obtained with a Finnigan LCQ Advantage max spectrometer.

Iron(III) chloride hexa-hydrate (98%), Iron(II) chloride tetrahydrate (99%), chlorosulfonic acid and other chemical materials were purchased from S.D. Fine Chemical Ltd., India. and tetra ethyl ortho silicate were purchased from sigma aldrich Chemicals. Anhydride and aniline were also purchased from S.D. Fine Chemical Ltd., India.

General procedure for preparation of catalyst:

$Fe_3O_4@SiO_2$ nanoparticles were prepared by the literature reported method[26,27]. Under nitrogen atmosphere, mixture of 5.0 g of ferric chloride and 1.85 g of ferrous chloride salts were dissolved in distilled water and heated to $90°C$. Then aqueous ammonia solution (25%) was added, from which precipitate of Fe_3O_4 was obtained. The supernatant was decanted and precipitate was isolated by magnetic separation. The obtained black powder (Fe_3O_4) was washed with acetone and dried under vacuum. The coating of silica on the surface of Fe_3O_4 nanoparticle was achieved, by diluting 2.0 g of Fe_3O_4 nanoparticle in water (40 ml), ethanol (120 ml) and aqueous ammonia solution (3.0 ml, 25%). The resultant dispersion was homogenised by sonicating it for 1 hr. at $40°C$. Then subsequently, tetraethyl orthosilicate diluted in ethanol was charged slowly under continuous mechanical stirring and further the mixture was stirred for 12 hr. The resultant brown powder was separated magnetically and washed three times with acetone and then dried.

The immobilization of sulfonic acid group on $Fe_3O_4@SiO_2$ was done by the literature reported method[28]. For preparation of sulfonic acid coated nano catalyst, mixture of silica coated magnetite (2.0 g) and 10 ml

of n-hexane was cooled. Chlorosulfonic acid (1.0 g) was added slowly to the above mixture over a period of 30 min at room temperature. The resulted sulfonic acid coated magnetic nano particles were separated and washed repeatedly with ethanol and dried in the oven at $60^{\circ}C$.

General procedure for synthesis of imide derivatives:

In a general procedure, mixture of phthalic anhydride (0.5g, 3.37 mmol), aniline (0.31g, 3.37 mmol) and $Fe_3O_4@SiO_2\text{-}SO_3H$ (0.1 g, 20 wt.%) in ethanol (5 ml) was stirred for 60 min at $80^{\circ}C$. After completion of the reaction (monitored by TLC), the catalyst was separated from the reaction mass by use of an external magnet. The organic layer was concentrated under reduced pressure to give the desired product which was subsequently purified in ethanol. The recovered catalyst was washed with acetone and dried at $60^{\circ}C$ to give recyclable $Fe_3O_4@SiO_2\text{-}SO_3H$. Yield 89%, 0.67 g, m.p. $208^{\circ}C$. All compounds were analysed by melting point, mass, IR and ^1H-NMR techniques.

Conclusion:

In conclusion, we have developed an efficient protocol for the synthesis of *N*-aryl phthalimide and biphenyl maleimide derivatives using sulphonic acid functionalised silica over magnetite Fe_3O_4 nanoparticles. These reactions were optimised for various parameters and have been employed for wide substrates. The advantages offered by this protocol include high TON values, easy separation method and recyclability of the catalyst up to six runs. This simple, efficient protocol can be explored for other organic synthesis in future as well.

Acknowledgment:

References:

1. L. M. Rossi, N. J. S. Costa, F. P. Silva, and R. Wojcieszak, *Green Chem.*, 2014, **16**, 2906.

2. R. Mrówczyński, A. Nan, and J. Liebscher, *RSC Adv.*, 2014, **4**, 5927.

3. M. Kawamura and K. Sato, *Chem. Commun.*, 2007, 3404–3405.

4. E. Rafiee, A. Ataei, S. Nadri, M. Joshaghani, and S. Eavani, *Inorg. Chim. Acta*, 2014, **409**, 302–309.

5. M. B. Gawande, A. K. Rathi, I. D. Nogueira, R. S. Varma, and P. S. Branco, *Green Chem.*, 2013, **15**, 1895–1899.

6. P. D. Stevens, J. Fan, H. M. R. Gardimalla, M. Yen, and Y. Gao, *Org. Lett.*, 2005, **7**, 2085–2088.

RSC Advances Accepted Manuscript

7.   V. Polshettiwar, B. Baruwati, and R. S. Varma, *Green Chem.*, 2009, **11**, 127–131.

8.   Y. Zheng, P. D. Stevens, and Y. Gao, *J. Org. Chem.*, 2006, **71**, 537–542.

9.   F.R. Benson, J.J. Ritter, *J. Am. Chem. Soc*. 1949, **71**, 4128–4129.

10.   S. M. Capitosti, T. P. Hansen, and M. L. Brown, *Bioorg. Med. Chem.*, 2004, **12**, 327–336.

11.   L. M. Lima, P. Castro, A. L. Machado, C. A. M. Fraga, C. Lugnier, V. L. G. de Moraes, and E. J. Barreiro, *Bioorg. Med. Chem.*, 2002, **10**, 3067–3073.

12.   A. A. Abdei-hafez, *Arch. Pharm. Res.*, 2004, **27**, 495–501.

13.   H. Sano, T. Noguchi, A. Tanatani, H. Miyachi, and Y. Hashimoto, *Chem. Pharm. Bull.*, 2004, **52**, 1021–1022.

14.   R. Jayakumar, R. Balaji, and S. Nanjundan, *Eur. Polym. J.*, 2000, **36**, 1659–1666.

15.   M.-D. Wu, M.-J. Cheng, B.-C. Wang, Y.-J. Yech, J.-T. Lai, Y.-H. Kuo, G.-F. Yuan, and I.-S. Chen, *J. Nat. Prod.*, 2008, **71**, 1258–1261.

16.   M. G. and B. G. John O. Osby, *Tetrahedron Lett.*, 1984, **25**, 2093–2096.

17.   C. D. Hurd and A. G. Prapas, *J. Org. Chem.*, 1959, **24**, 388–392.

18.   M. A. Walker, *J. Org. Chem.*, 1995, **60**, 5352–5355.

19.   D. C. Chen, H. Q. Ye, and H. Wu, *Catal. Commun.*, 2007, **8**, 1527–1530.

20.   M.-Y. Zhou, Y.-Q. Li, and X.-M. Xu, *Synth. Commun.*, 2003, **33**, 3777–3780.

21.   M. N. Mo, N. Bundaleski, A. Santos, M. N. D. Teodoro, and R. Luque, *Green Chem.*, 2013, **15**, 682–689.

22.   E. Rafiee and S. Eavani, *Green Chem.*, 2011, **13**, 2116–2122.

23.   H. Naeimi and S. Mohamadabadi, *Dalton Trans.*, 2014, **43**, 12967–73.

24.   M. Yamaura, R. . Camilo, L. . Sampaio, M. . Macêdo, M. Nakamura, and H. . Toma, *J. Magn. Magn. Mater.*, 2004, **279**, 210–217.

25.   R. Rahimi, A. Maleki, and S. Maleki, *Chinese Chem. Lett.*, 2014, **25**, 919–922.

26.   K. Yang, H. Peng, Y. Wen, and N. Li, *Appl. Surf. Sci.*, 2010, **256**, 3093–3097.

27.   D. Yang, J. Hu, and S. Fu, *J.Phys.Chem.C*, 2009, **113**, 7646–7651.

28.   F. Nemati, M. Heravi, and R. S. RAD, *Chinese J. Catal.*, 2012, **33**, 1825–1831.
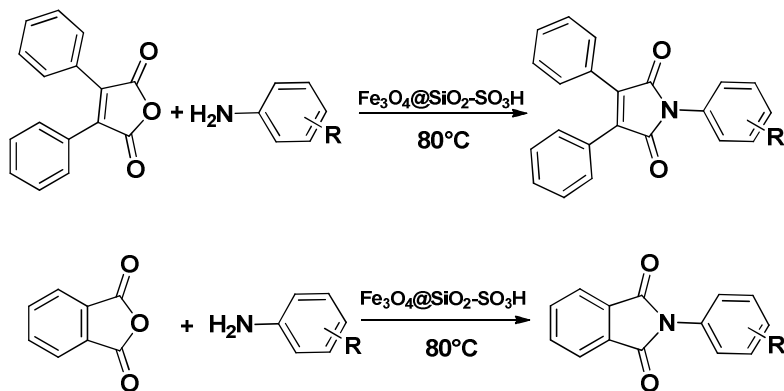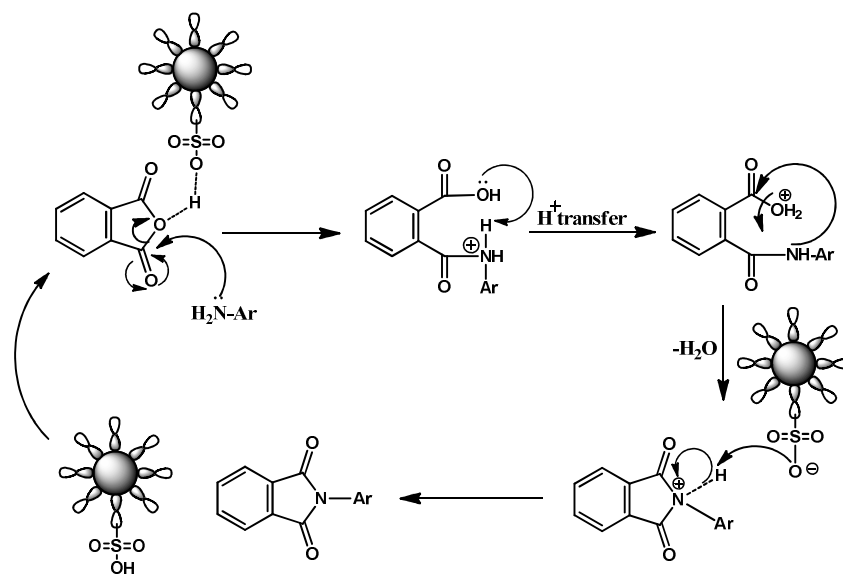
Figure Captions:

Scheme1:

Figure 1: Proposed reaction mechanism.

Figure 2: (a) SEM and (b) TEM images of $Fe_3O_4@SiO_2$-SO_3H catalyst.

Figure 3: XRD spectra of (a) Fe_3O_4, (b) $Fe_3O_4@SiO_2$ and (c) $Fe_3O_4@SiO_2$-SO_3H.
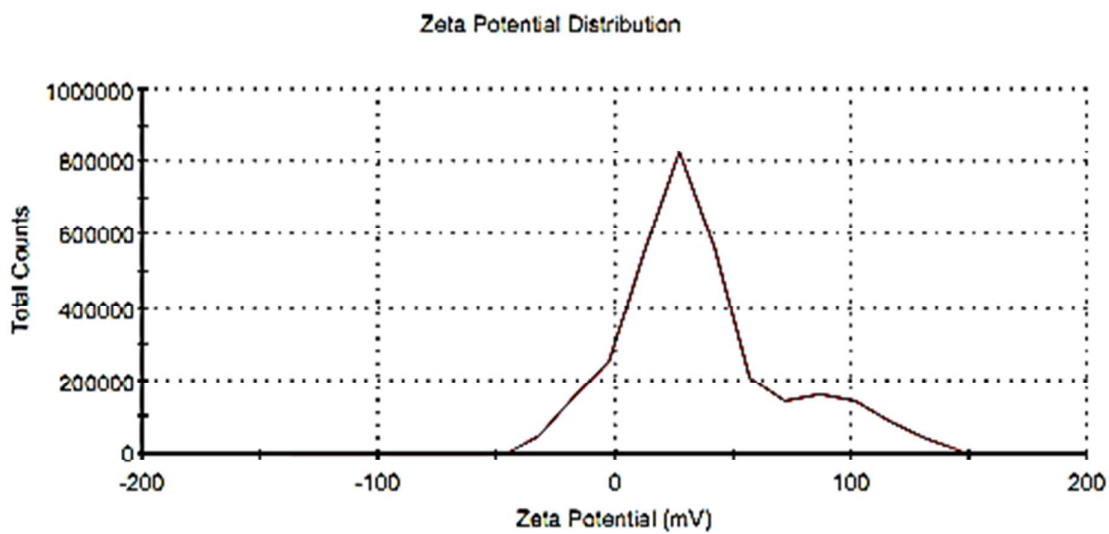
Figure 4: Zeta potential of $Fe_3O_4@SiO_2$-SO_3H.
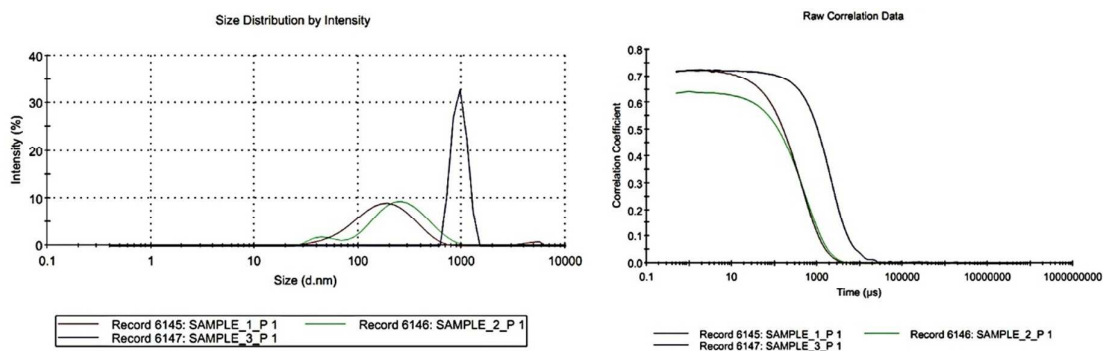
Figure 5: DLS measurement of (1) Fe_3O_4 (2) $Fe_3O_4@SiO_2$ and (3) $Fe_3O_4@SiO_2$-SO_3H.
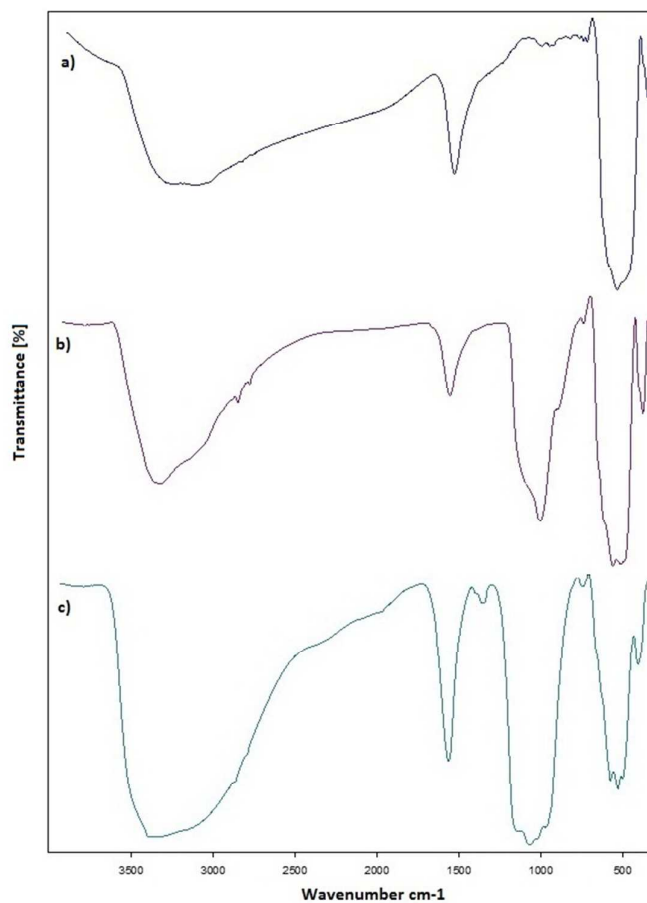
Figure 6: FT-IR spectra of (a) Fe_3O_4, (b) $Fe_3O_4@SiO_2$ and (c) $Fe_3O_4@SiO_2$-SO_3H.

Figure 7: Recyclability study of $Fe_3O_4@SiO_2$-SO_3H in the synthesis of *N*-phenyl phthalimide.

Fig: 8 (a) SEM and (b) TEM images of recovered catalyst after six successive runs of reaction.

Scheme1:

Where R= H, -Cl,-F,-OCH₃,-CH₃, NO₂ etc

Figure 1: Proposed reaction mechanism.

Figure 2: (a) SEM and (b) TEM images of $Fe_3O_4@SiO_2$-SO_3H catalyst.

2

Figure 3: XRD spectra of (a) Fe_3O_4, (b) $Fe_3O_4@SiO_2$ and (c) $Fe_3O_4@SiO_2-SO_3H$.

Figure 4: Zeta potential of $Fe_3O_4@SiO_2-SO_3H$.

3

Figure 5: DLS measurement of (1) Fe_3O_4, (2) $Fe_3O_4@SiO_2$ and (3) $Fe_3O_4@SiO_2-SO_3H$.

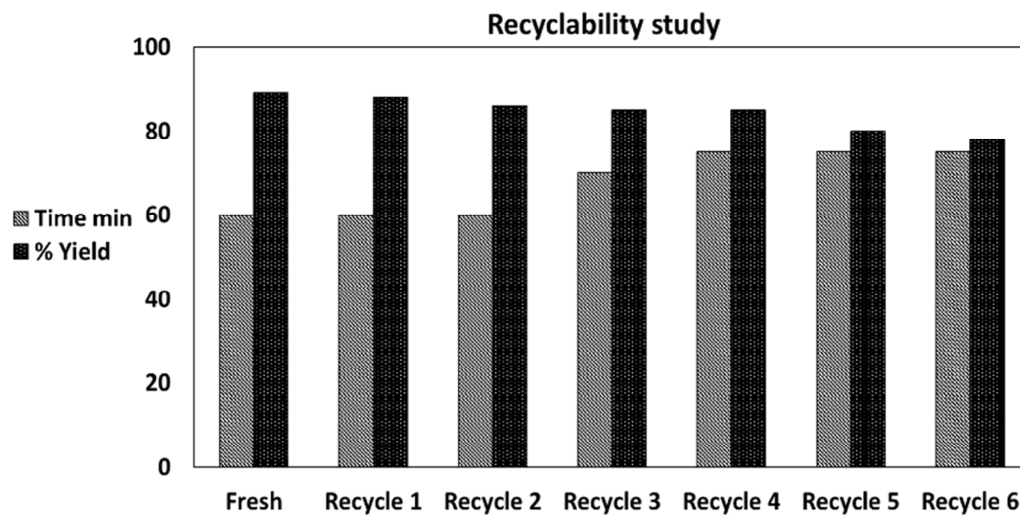Figure 6: FT-IR spectra of (a) Fe_3O_4, (b) $Fe_3O_4@SiO_2$ and (c) $Fe_3O_4@SiO_2-SO_3H$.

4

Figure 7: Recyclability study of Fe_3O_4@SiO_2-SO_3H in the synthesis of *N*-phenyl phthalimide.
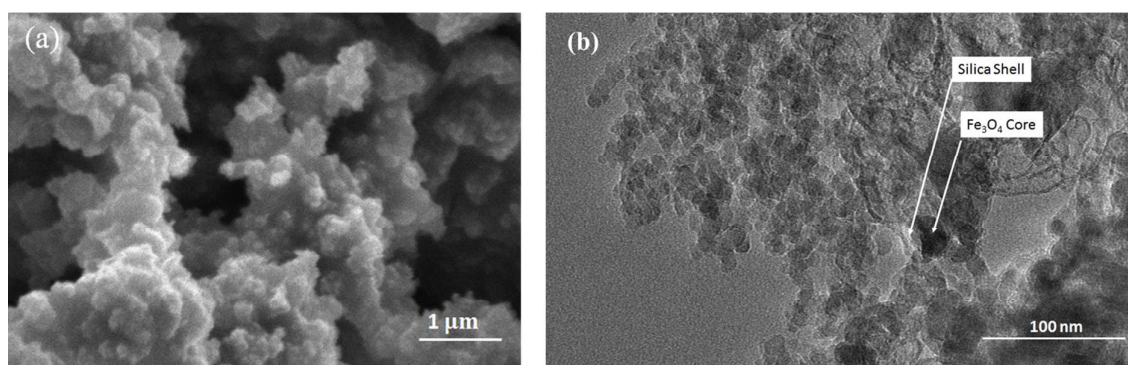

Fig: 8 (a) SEM and (b) TEM images of recovered catalyst after six successive runs of reaction.

Graphical abstract: